BOREAL ENVIRONMENT RESEARCH 19 (suppl. B): 293–310 © 2014
ISSN 1239-6095 (print) ISSN 1797-2469 (online) Helsinki 30 September 2014

Monoterpenes' oxidation capacity and rate over a boreal forest: temporal variation and connection to growth of newly formed particles

Otso Peräkylä[1)], Matthias Vogt[1)], Olli-Pekka Tikkanen[1)], Terhi Laurila[1)], Maija K. Kajos[1)], Pekka A. Rantala[1)], Johanna Patokoski[1)], Juho Aalto[2)], Taina Yli-Juuti[1)], Mikael Ehn[1)], Mikko Sipilä[1)], Pauli Paasonen[1)3)], Matti Rissanen[1)], Tuomo Nieminen[1)], Risto Taipale[1)], Petri Keronen[1)], Hanna K. Lappalainen[1)], Taina M. Ruuskanen[1)], Janne Rinne[1)4)], Veli-Matti Kerminen[1)], Markku Kulmala[1)], Jaana Bäck[2)] and Tuukka Petäjä[1)]

[1)] *Department of Physics, P.O. Box 64, FI-00014 University of Helsinki, Finland*
[2)] *Department of Forest Sciences, P.O. Box 27, FI-00014 University of Helsinki, Finland*
[3)] *Finnish Environment Institute, Centre for Sustainable Consumption and Production, P.O. Box 140, FI-00251 Helsinki, Finland*
[4)] *Department of Geosciences and Geography, P.O. Box 64, FI-00014 University of Helsinki, Finland*

Received 15 Nov. 2013, final version received 16 Apr. 2014, accepted 16 Apr. 2014

Peräkylä, O., Vogt, M., Tikkanen, O.-P., Laurila, T., Kajos, M. K., Rantala, P. A., Patokoski, J., Aalto, J., Yli-Juuti, T., Ehn, M., Sipilä, M., Paasonen, P., Rissanen, M., Nieminen, T., Taipale, R., Keronen, P., Lappalainen, H. K., Ruuskanen, T. M., Rinne, J., Kerminen, V.-M., Kulmala, M., Bäck, J. & Petäjä, T. 2014: Monoterpenes' oxidation capacity and rate over a boreal forest: temporal variation and connection to growth of newly formed particles. *Boreal Env. Res.* 19 (suppl. B): 293–310.

The subject of the study was the effect of monoterpene oxidation on the growth of particles during new-particle formation (NPF) events at the SMEAR II measurement station in Hyytiälä, southern Finland, during 2006–2011. The nighttime oxidation capacity, i.e. how readily the atmosphere can oxidize monoterpenes, was found to be dominated by the nitrate radical, whereas the daytime oxidation capacity was mainly dominated by ozone. The mean lifetimes of monoterpenes ranged from about one hour to several hours, depending on the time of year and day. A strong link was found between the growth rate of particles of 7–20 nm in diameter during the NPF events and monoterpene oxidation by ozone during the preceding night. Our findings suggest that during nighttime a build-up of primarily oxidized monoterpenes in the atmosphere occurs, and that these compounds can be oxidized by the hydroxyl radical after sunrise, promoting the particle growth.

Introduction

Biogenic volatile organic compounds (biogenic VOCs) affect the atmospheric chemistry as well as the formation and growth of aerosol particles (Kulmala *et al*. 1998, Atkinson and Arey 2003, Tunved *et al*. 2006, Paasonen *et al*. 2013). The largest group of volatile organic compounds emitted by the boreal forests are monoterpenes (Rinne *et al*. 2009). They have various molecular structures, but share the molecular formula $C_{10}H_{16}$ and therefore have the same molecular

Editor in charge of this article: Hannele Korhonen

mass. Monoterpenes are among the most studied biogenic VOCs, and they are produced and emitted by many boreal tree species, including *Pinus sylvestris*, *Picea abies*, *Betula pubescens* and *Betula pendula* (Isidorov *et al*. 1985, Rinne *et al*. 2009, Bäck *et al*. 2012). The emissions can originate either directly from synthesis, or from permanent storages (Ghirardo *et al*. 2010). In addition, monoterpene emissions can be related to defence mechanisms (Litvak *et al*. 1999) or release from storage pools by a mechanical injury.

Monoterpene emissions depend mainly on the temperature (Guenther *et al*. 2012), so they are emitted also during nighttime. Since the planetary boundary layer is the shallowest during night, also the highest above-canopy monoterpene concentrations are being recorded during that time of the day (Hakola *et al*. 2012).

Monoterpenes and other VOCs can be removed from the atmosphere by their reaction with various oxidants. The oxidation products of these reactions generally have a lower volatility and they are characterised by higher oxygen-to-carbon (O:C) ratios than the reactant VOCs (Donahue *et al*. 2012). They can therefore condense onto various surfaces and hence be removed from the atmosphere. The most important oxidants in the atmosphere are ozone (O_3), hydroxyl radical (OH•, hereafter OH) and nitrate radical (NO_3•, hereafter NO_3).

Atmospheric aerosol particles originate from either direct particle emissions to the atmosphere (primary particles) or formation of new particles by nucleation of low-volatility vapours (secondary particles). Around the world, bursts of particle formation by nucleation, i.e. new-particle formation (NPF) events, have been observed (Kulmala *et al*. 2004). Sulphuric acid, which is also related to atmospheric oxidation, has been estimated to be important in the formation of these particles (Sipilä *et al*. 2010). The particles formed recently by nucleation are small, in the nanometre size range. To be climatically relevant, newly-formed particles need to grow to sizes larger than about 50–100 nm in diameter (Kerminen *et al*. 2012). In this growth process, condensation of VOC oxidation products has been estimated to play a large role (Kulmala *et al*. 1998, Riipinen *et al*. 2012, Paasonen *et al*. 2013).

In this study, the connection of monoterpene concentrations and oxidation with new-particle formation, especially the growth rate of the formed particles, was studied. The main goal of the paper was to find out how the oxidation of monoterpenes affects the growth rate of particles formed by nucleation during new-particle formation events. The specific questions addressed here were: How do the oxidant concentrations, as well as the oxidation capacity (i.e. how readily the atmosphere oxidizes any available monoterpenes) caused by the oxidants, vary temporally? How long are the atmospheric lifetimes of monoterpenes with respect to oxidation reactions? How do the monoterpene concentrations vary temporally? What is the relation of monoterpene concentrations, as well as the oxidant concentrations and these two combined, to the growth rates of different sized particles during new-particle formation events?

The temporal variation of the oxidant gases was investigated, along with the oxidation capacity of the atmosphere with respect to monoterpenes. The data on oxidant and monoterpene concentrations were then compared with observed growth rates of nanoparticles during NPF events.

Material and methods

Measurement site

The measurements were conducted at the SMEAR II station of the University of Helsinki in Hyytiälä, southern Finland (Station for Measuring Forest Ecosystem–Atmosphere Relations, 61°51´N, 24°17´E, 181 m a.s.l.). SMEAR II is a rural measurement site located in a rather homogenous Scots pine (*Pinus sylvestris*) forest sown in 1962. In addition to Scots pine, there are some Norway spruce (*Picea abies*), trembling aspen (*Populus tremula*) and birch (*Betula* spp.). The undergrowth of the forest consists of heather (*Calluna vulgaris*), lingonberry (*Vaccinium vitis-idaea*), blueberry (*Vaccinium myrtillus*), wavy hairgrass (*Deschampsia flexuosa*) and mosses (*Pleurozium schreberi*, *Dicranum* sp.). The annual mean temperature is 3 °C with the coldest month being January (mean –9 °C) and the warmest July (mean 15 °C). The annual mean

precipitation is 700 mm. The station provides continuous measurements of trace gas concentrations, aerosol particle number size distributions, and meteorological quantities like temperature and radiation, and ecosystem functioning including carbon, water and nitrogen fluxes and emissions of volatile organic compounds. (Hari and Kulmala 2005, Ilvesniemi *et al*. 2010).

Experimental setup

Volatile organic compounds

The volume mixing ratios (VMRs) of the volatile organic compounds were measured with a quadrupole proton transfer reaction mass spectrometer (PTR-MS, Ionicon Analytik GmbH, Austria). The measurements were conducted non-continuously between 2006 and 2009, and from 2009 onwards on a continuous basis with periodic interruptions during maintenance and instrument malfunctioning.

The PTR-MS is an instrument which allows for real-time measurements of VMRs down to tens of ppt (parts per trillion) range. The sample air is pumped continuously through a drift tube reactor, where the VOCs of the sample air are ionized in a proton transfer reaction with hydronium ions (H_3O^+). The advantage of the H_3O^+ ion is that it performs a non-dissociative proton transfer to a majority of the VOCs, but does not react with the constituents of clear air. After the drift tube, the ions are guided to a quadrupole mass spectrometer for the selection and detection of the reagent and product ions. As the quadrupole PTR-MS measures with a one Thomson (Th) resolution, different compounds with same nominal mass cannot be distinguished, and it cannot be used for identification of e.g. individual monoterpenes [for more details about the instrument, *see* Lindinger *et al*. (1998), deGouw *et al*. (2003), Warneke *et al*. (2003) and deGouw and Warneke (2007)].

The measurement setup, the volume mixing ratio calculations and used calibration procedure have been described in detail by Taipale *et al*. (2008), so here we give only a short description. Until July 2009, the sampling height was 14 meters, i.e. close to the top of canopy (tree height in 2009 16.5 m). The sample air was carried to the instrument via a 30-m-long PTFE tubing (inner diameter 8 mm) with a continuous flow of about 18 l min^{-1}. Between May 2006 and March 2007, the VMR measurements were made every second hour as the same instrument was used for ecosystem-scale VOC flux measurements that were made during the other hours (Rinne *et al*. 2007, Taipale *et al*. 2011). In April 2007, the measurements were changed so that also Scots pine shoot emission measurements were added to the measurement cycle (Kolari *et al*. 2012), thus VMR measurements were then made every third hour.

In 2010, the VMR sampling was moved to another tower about 20 m away from the old sampling place, and at the same time the sampling height was changed to 16.8 m. The volume mixing ratio measurements were still made every third hour with the other two hours allocated for shoot and soil emission measurements.

In order to determine the instrumental background, VOC-free air was measured variably every second or third hour. The VOC-free air was produced by pumping outdoor air through a catalytic converter (Parker Balston zero air generator HPZA-3500, USA). A three-way valve was used to switch the sampling between the ambient air and zero air. The PTR-MS was calibrated every second week with a standard gas mixture. During the measurement period, we had four different gas standards (all made by Apel-Riemer Environmental Inc., USA) consisting of 16–18 different VOCs. The monoterpenes were calibrated using α-pinene as the standard.

Oxidants

The ozone concentration was measured with an ultraviolet light absorption analyser (TEI 49C, Thermo Fisher Scientific, Waltham, MA, USA). The measurements were carried out from the mast at a variety of heights ranging from 4.2 to 67.2 m above the mast base. Measurements from the 16.8-m height were used as 30-minute average values. Unless otherwise mentioned, all the other measurements were also used as 30-minute averages. The detection limit of the instrument is one part per billion (ppb) and the relative accuracy is ±3%.

The UVB radiation intensity used for calculating the hydroxyl radical concentration was measured at the 18-m height by a SL 501A UVB pyranometer (Solar Light, Philadelphia, PA, USA).

The concentrations of nitrogen oxide (NO) and NO_x ($NO + NO_2$), used in calculating nitrate radical production were measured using a chemiluminescence analyser (TEI 42C TL, Thermo Fisher Scientific, Waltham, MA, USA). The detection limit of the instrument is 0.1 ppb and its relative accuracy ±10%. The data under the detection limit, including negative values, were changed to zero. The concentration of NO_2 was calculated as the difference of measured NO_x and NO concentrations. Until 27 February 2007, a molybdenum converter was used to convert NO_2 to NO for the measurement of NO_x. This also converted other reactive nitrogen species, such as peroxyacyl nitrates, to NO. Therefore, the concentration of NO_2 should be regarded as an upper limit for the actual concentration until that time. From 1 March 2007, a specific photolytic converter (Blue Light Converter, Droplet Measurement Technologies, Boulder, CO, USA) was used for converting NO_2 to NO, removing this interference.

Aerosol surface area

The aerosol size distributions measured with a twin Differential Mobility Particle Sizer (DMPS) system (Aalto *et al*. 2001) were used for calculating the aerosol surface area, which was used in the calculation of the lifetime of the nitrate radical. The particle number size distribution in the diameter range 3–1000 nm has been measured since December 2004. Before that the size range was 3–600 nm, but these data were not used in this paper.

Calculation of the particle growth rate

The growth rates (GR) of aerosol particles and ions were calculated using the maximum concentration method presented by Hirsikko *et al*. (2005) and Yli-Juuti *et al*. (2011). When particles grow during a new-particle formation event day, local maxima are found in the time series of concentration of nucleation mode particles. The value of GR is calculated based on the difference in time when the maximum is found from different size fractions.

The growth rate was obtained as the slope of a linear function fitted to the data pairs of the times when the concentration peaks, and the corresponding geometric mean diameters. The linear function was fitted for three different size ranges, provided that there were at least three data points in that size range. These size ranges correspond to the mobility diameters of 1.5–3 nm, 3–7 nm and 7–20 nm.

The GR was calculated based on particle and ion size measurements with the DMPS, Balanced Scanning Mobility Analyzer (BSMA; Tammet 2006), Air Ion Spectrometer (AIS, from 2006 to 2007; Mirme *et al*. 2007) and Neutral cluster and Air Ion Spectrometer (NAIS, from 2010 onwards; Kulmala *et al*. 2007). The GR from the DMPS measurements was calculated only for the size ranges 3–7 nm and 7–20 nm, and from the BSMA measurements for the size ranges 1.5–3 nm and 3–7 nm, based on the measurement size ranges of these two devices. The GR from the AIS and NAIS was calculated for all the three size ranges. Finally, the growth rates calculated based on different instruments were averaged to obtain a single value, which then represented the GR of that size range on that specific day.

Yli-Juuti *et al*. (2011) investigated the differences in the growth rates calculated from the different instruments. According to their results, the instruments generally agree fairly well in the calculated values of the growth rates. In the smallest size class, 1.5–3 nm, the AIS/NAIS gives consistently higher growth rates than the BSMA. When looking at the two other size classes, such a systematic difference is not observed. A random variability (i.e. the non-systematic differences) between the growth rates calculated based on different instruments also decreases with an increasing particle size.

There are two main sources of uncertainties related to the maximum concentration method discussed in more detail by Yli-Juuti *et al*. (2011). In short, a sudden change in the air mass causes the peak in the concentration time series

to be narrower than what would be expected, which then causes the calculated GR to be higher than the true value. Also the fluctuation in the growing nucleation particle mode might sometimes cause more than one peak in the concentration time series, in which case it is not clear which peak to choose and the method is prone to subjective error. In total, the GR obtained using this method more likely overestimates the actual GR than underestimates it (Yli-Juuti *et al*. 2011).

Using charged particles instead of neutral ones, or the sum of both, might also result in some error in the growth-rate calculation, such that the calculated growth rate does not represent the whole aerosol population (Leppä *et al*. 2013). This effect varies from case to case, and therefore cannot be accounted for in the calculation. Also, coagulation may influence the growth rate when the nucleation mode number concentration is high, in which case the growth rate does not represent the growth by condensation (Leppä *et al*. 2011). This effect should, however, be small as the nucleation mode concentrations in Hyytiälä were low.

Estimating the oxidation capacity

The concept of oxidation capacity was adapted from Geyer *et al*. (2001a) and used here for monoterpenes. The oxidation capacity of the atmosphere with respect to a specific substance was defined here by summing the products of concentrations of the oxidant gases with their reaction rate coefficients with the substance in question. Thus, the oxidation capacity is a measure of how readily the atmosphere oxidizes any of the available substance. In a steady state between the production and removal of the substance, the oxidation capacity also becomes the inverse of its turnover time and mean lifetime (τ_{SS}).

For monoterpenes (MT), the oxidation capacity (OCAP) is defined as

$$\mathrm{OCAP}_{\mathrm{MT}} = k_{\mathrm{OH+MT}}[\mathrm{OH}] + k_{\mathrm{O_3+MT}}[\mathrm{O_3}] + k_{\mathrm{NO_3+MT}}[\mathrm{NO_3}], \quad (1)$$

where k is the average reaction rate coefficient of the oxidant (OH, O_3 or NO_3) with monoterpenes, and the concentration of the oxidant is given brackets. Monoterpenes are a broad group of compounds, each with different chemical properties and individual reaction rate coefficients (Atkinson 1997). The data for individual monoterpene concentrations at the station was available only as monthly-mean values (Hakola *et al*. 2012). Therefore, mean reaction rate coefficients weighted with the individual monoterpene fractions (k_{monthly}) were used for each month. The average reaction rate coefficients were calculated by using the following equation:

$$k_{\mathrm{monthly}} = \sum f_i k_i, \quad (2)$$

where f_i is the monthly fraction of monoterpene i and k_i is its reaction rate coefficient with the oxidant gas in question. The reaction rate coefficients of O_3 and OH with individual monoterpenes, as well as monthly fractions of the most abundant monoterpenes measured in Hyytiälä reported by Hakola *et al*. (2012), were used. For the reaction rate coefficients of monoterpenes with NO_3, the data reported by Atkinson (1997) were used. The data for individual monoterpene concentrations were only available for a bit more than one year, and for many months the concentrations were below the detection limit. Therefore, the reaction rates of each month were smoothed using a running mean of the reaction rate calculated for the actual month and the reaction rates for the months before and after this month. The actual month was weighted by the factor of two.

The monoterpene composition changes seasonally, α-pinene being the most abundant monoterpene in summer, while camphene and other monoterpenes dominate in winter. A more detailed discussion on the varying monoterpene composition is given in Hakola *et al*. (2012). Due to the changing monoterpene composition, the average reaction rate coefficient of monoterpenes with NO_3 varied the most (Table 1), being the highest (7.5×10^{-12} molecules cm^{-3} s^{-1}) in July and the lowest (2.2×10^{-12} molecules cm^{-3} s^{-1}) in January. The reaction rate coefficient with ozone varied in a similar way with the peak in July and the lowest value in January. The reaction rate coefficients with OH varied less, yet the highest value was in July and lowest one in January.

The ozone concentration used in the calculation of the oxidation capacity was measured

directly as described earlier. The hydroxyl radical concentration was not measured directly, but it correlates strongly with the UVB radiation intensity (Röhrer and Berresheim 2006) and was calculated from the measured UVB radiation intensity using a proxy adapted from Petäjä *et al*. (2009):

$$[OH]_{proxy} = 5.62 \times 10^5 \times UVB^{0.62}. \quad (3)$$

Due to the method used, the calculated hydroxyl radical concentration was zero during the night when there was no UVB radiation.

The nitrate radical was not measured directly. It is formed in the reaction of ozone and nitrogen dioxide:

$$O_3 + NO_2 \rightarrow NO_3 + O_2. \quad (4)$$

The concentration of the nitrate radical was calculated assuming a steady state between its production and removal:

$$[NO_3]_{steady\text{-}state} = J_{NO_3}\tau_{NO_3}, \quad (5)$$

where J_{NO_3} is the production rate of NO_3, and τ_{NO_3} is its lifetime. The production rate was calculated from the reaction between NO_2 and ozone:

$$J_{NO_3} = k_{O_3 + NO_2}[O_3][NO_2]. \quad (6)$$

The temperature (T)-dependent reaction rate coefficient $k_{O_3 + NO_2}$ of $1.4 \times 10^{-13}\exp(-2470/T)$ was used (Vrekoussis *et al*. 2004).

During daytime the nitrate radical is rapidly photolysed by solar radiation with an estimated lifetime of five seconds for overhead sun (Orlando *et al*. 1993, Vrekoussis *et al*. 2004). This lifetime was used for all times when the UVB radiation exceeded 0.01 W m^{-2}. In addition to being photolysed, nitrate radical undergoes oxidation reactions with hydrocarbons. Its main hydrocarbon sinks in the boreal forest are monoterpenes and isoprene, C_5H_8. Isoprene was also measured with the PTR-MS. The nitrate radical also reacts with NO_2 to produce N_2O_5 in an equilibrium reaction according to

$$NO_3 + NO_2 \leftrightarrow N_2O_5. \quad (7)$$

N_2O_5 can then react with atmospheric water vapour, or be taken up by aerosol surfaces. These reactions hence constitute an effective removal pathway of NO_3 through the equilibrium reaction.

Nitrate radical also reacts with NO which is a free radical. It is produced photochemically and has a short lifetime with respect to reactions with ozone. However, if there are additional local sources (such as the soil), it can also take part in the nocturnal removal of NO_3 (Geyer *et al*. 2001b).

For the lifetime of NO_3 during nighttime, an upper limit was calculated according to Allan *et*

Table 1. The smoothed montly-mean reaction rate coefficients for the reaction of monoterpenes with the oxidants O_3, OH and NO_3. The reaction rates vary with the changing monoterpene composition: the individual monoterpene concentration data used in calculation were taken from Hakola *et al.* (2012).

	$k_{O_3 + MT}$ ($\times 10^{-17}$ cm^{-3} s^{-1})	$k_{OH + MT}$ ($\times 10^{-11}$ cm^{-3} s^{-1})	$k_{NO_3 + MT}$ ($\times 10^{-12}$ cm^{-3} s^{-1})
January	2.1	5.1	2.2
February	3.3	5.1	3.1
March	4.4	5.2	4.1
April	5.3	5.7	4.9
May	6.8	6.1	5.4
June	6.3	6.6	6.3
July	6.9	7.4	7.5
August	6.8	7.3	7.0
September	6.3	6.8	6.2
October	5.7	6.6	5.5
November	4.8	6.5	4.5
December	3.1	5.8	3.0
Mean	5.0	6.2	5.0

al. (2000), with the addition of the reaction with nitric oxide:

$$(\tau_{NO_3})^{-1} = k_{NO_3 + MT}[MT] + k_{NO_3 + isop.}[isop.] + k_{NO_3 + NO}[NO] + (k_{N_2O_5 + H_2O}[H_2O] + k_{het(N_2O_5)}) \times K[NO_2], \quad (8)$$

where K is the equilibrium constant for Eq. 7, for which the temperature-dependent value of $5.1 \times 10^{-27}\exp(10871/T)$ was used (Osthoff *et al*. 2007). The equilibrium constant therefore increases with a decreasing temperature. For the reaction rate coefficients of isoprene and nitric oxide with NO_3, the values $3.03 \times 10^{-12}\exp(-450/T)$ by Dlugokencky and Howard (1989) and $1.8 \times 10^{-11}\exp(110/T)$ from the Master Chemical Mechanism (MCM; Jenkin *et al*. 2003, Saunders *et al*. 2003) were used, respectively. In Eq. 8, $k_{het(N_2O_5)}$ is the reaction rate coefficient for the heterogeneous uptake of N_2O_5 to aerosol surfaces. This is defined by the following equation:

$$k_{het} = 0.25Ac\gamma, \quad (9)$$

where A is the aerosol surface area in $cm^2\ cm^{-3}$, c is the root mean square speed of the N_2O_5 molecules in cm s^{-1}, and γ is the heterogeneous uptake coefficient for N_2O_5. For γ, the value 4×10^{-4} from the MCM was used.

The VOC measurements required for calculating the lifetime in Eq. 8 were not continuous for the whole period, and they were of lower resolution as compared with the other gas measurements. They were available only for about 10% of the data points, but these data were spread out throughout the study period. Accordingly, the sink term and the NO_3 concentration could only be calculated for that fraction of the data points.

Estimating the oxidation rate of monoterpenes

The oxidation of monoterpenes in the atmosphere is a first-order reaction with respect to all the reactants, so it depends linearly on the reactant concentrations. The oxidation rate (OR) of monoterpenes in the atmosphere can therefore be calculated by multiplying the oxidation capacity with respect to monoterpenes ($OCAP_{MT}$) by the concentration of monoterpenes:

$$OR_{MT} = OCAP_{MT}[MT]. \quad (10)$$

Results

Oxidant concentrations

The O_3 concentration peaked in spring, being the highest in April and May (Fig. 1a). Within those months, and from March to September, the concentration was clearly the highest during the afternoon, with the highest median concentrations being around 1×10^{12} molecules cm^{-3}. The lowest concentrations, being around 5×10^{11} molecules cm^{-3}, were observed in the early morning during September. It is notable that the maximum median concentrations were only around two times higher than the minimum median values.

The calculated OH concentration followed the cycle of sunlight. It can be seen that the proxy OH concentration peaked during summer in midday when the median concentration was around 8×10^5 molecules cm^{-3} (Fig. 1b). Year round, the OH concentration calculated by proxy was the lowest during nighttime when it decreased to zero as it was calculated from the UVB radiation. The daily-average OH concentration was the lowest in the winter when little sunlight is available.

When comparing the measured UVB radiation with the daytime OH concentration measured in 2007 in Hyytiälä, Petäjä *et al*. (2009) found that the two quantities were relatively strongly correlated ($r = 0.76$). Also, the magnitude of the measured daytime OH concentration was similar to the proxy concentration (Petäjä *et al*. 2009), justifying the use of a proxy for the daytime OH concentration. During nighttime, the measured OH concentrations were about an order of magnitude lower than the measured daytime concentrations (Petäjä *et al*. 2009), and the concentrations calculated by proxy decreased to zero. However, the nighttime oxidation capacities resulting from the measured OH concentrations would be of the order of 10^{-6} s^{-1}. The calculated nighttime oxidation capacity due to O_3 and NO_3 was of the order of 10^{-4} s^{-1}, i.e. two orders

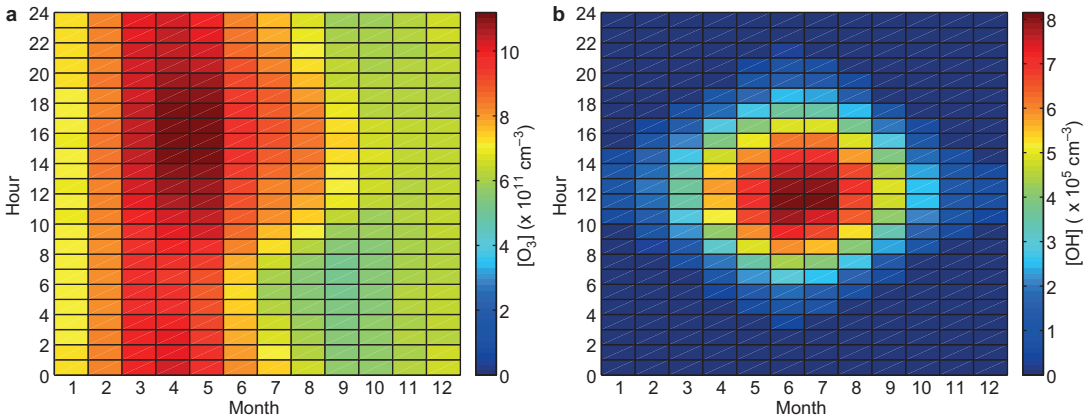

Fig. 1. Temporal variations in the concentrations of oxidants (**a**) O_3 and (**b**) OH (calculated) averaged over the period 2006–2011. The times are UTC + 2 h. Colouring indicates the median concentration of the oxidant gas in question during the hours given by *y*-axis in the month given by *x*-axis. The set of values for each month therefore represents the median diurnal cycle for that month.

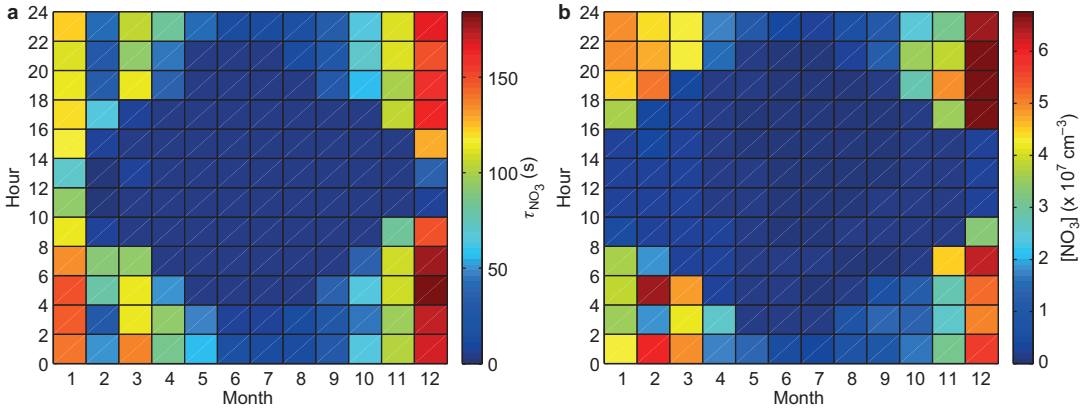

Fig. 2. Temporal variations in the (**a**) median calculated lifetime and (**b**) concentration of NO_3. Due to fewer data available, the diurnal cycles are averaged over two-hour intervals (one hour for the other two oxidants in Fig. 1).

of magnitude higher (*see* section 'Oxidation capacity' below). Therefore, omitting nighttime OH concentrations should not cause large errors in calculating the oxidation capacity and rate. In summer when the nighttime oxidation capacity was the lowest, the OH concentration might have a non-negligible effect on the nighttime oxidation capacity. However, the oxidation capacity due the other two oxidants would still be clearly higher. Therefore, using the proxy is justified, yet it should be kept in mind that OH concentrations were non-zero even during nights.

During daytime, the calculated lifetime of NO_3 was always short (set to 5 s) due to photodissociation (Fig. 2a). The shortest nighttime lifetimes of NO_3 were observed from late spring to autumn, the smallest median value being 6 s and typically values of a few tens of seconds. NO_3 oxidizes VOCs, mainly monoterpenes, rapidly and its lifetime with respect to the VOC reactions is short. From May to September, the median contribution of VOC reaction to the total the nighttime NO_3 loss was > 98%, when all the data points covering this period were taken into account. The longest nighttime lifetimes of NO_3, between 100 and 200 s, were observed in December. At this time of the year, the lifetime of NO_3 with respect to its reaction with monoter-

penes was the longest, yet the reactions between NO_3 and VOCs were responsible, on average, for 79% of the total NO_3 loss. The lifetime of NO_3 associated with the loss of N_2O_5 on aerosol surfaces or by water vapour was almost always longer than its lifetime associated with its reaction with monoterpenes. The exception was February, when monoterpene concentrations were low and the reaction of N_2O_5 with water vapour dominated the sink term (contribution of water to the sink term was 51%, and VOCs 22%).

The calculated NO_3 concentration followed mainly the pattern of the calculated NO_3 lifetime (Fig. 2). During daytime, the lifetime of NO_3 was always short and its concentration was low, around 10^6 molecules cm^{-3}. In this respect NO_3 showed behaviour opposite to that of the proxy OH concentration.

The production rate of NO_3 according to Eq. 6 was the highest during the winter–spring period, showing a peak in February. The highest daily values were obtained at around 18:00. This was caused by the overlapping high concentrations of ozone and nitrogen dioxide, of which the latter peaks in February. The lowest NO_3 production rates were obtained during summer and autumn, with a diurnal minimum after midday in summer and early morning in autumn. The low production rate was mainly due to the low nitrogen dioxide concentrations in the summer, and low ozone concentrations in the autumn. The highest median proxy NO_3 concentrations of about 6×10^7 molecules cm^{-3} were obtained in December when the NO_3 lifetime was the longest.

The nighttime nitrate radical concentration was measured during the HUMPPA-COPEC campaign from 12 July to 12 August 2010 (Williams *et al*. 2011), but for the entire campaign the concentration was below the detection limit of 2×10^7 molecules cm^{-3} (Rinne *et al*. 2012). This agreed with the calculated NO_3 concentration which was mostly below 5×10^6 molecules cm^{-3} for the same period, the maximum value being 9×10^6 molecules cm^{-3}.

Vrekoussis *et al*. (2004) listed nitrate radical concentrations measured in the continental and marine boundary layer at various locations. Generally, the concentrations were a few pptv (Vrekoussis *et al*. 2004, and references therein), which translates to around $1–3 \times 10^8$ molecules cm^{-3}. Out of the sites listed, the only continental one is the rural site in Lindenberg (Germany), where the nitrate radical concentration was measured by Geyer *et al*. (2001a). In their study, the average concentration of the nitrate radical was 5.7 pptv ($\approx 1.4 \times 10^8$ molecules cm^{-3}) in May–September, and the average NO_3 lifetime was 130 seconds. The concentrations reported by Geyer *et al*. (2001a) are higher than the maximum values calculated in this study, but the lifetimes are of the same order of magnitude. Geyer *et al*. (2001a) found that the average production rate of NO_3 from NO_2 and O_3 was 1.1×10^6 molecules cm^{-3} s^{-1}, which is about three times higher than the production rate calculated in this study (3.3×10^5 molecules cm^{-3} s^{-1}) for the same months. Hence, the lower NO_3 concentrations at our site were at least partly caused by the lower concentrations of the precursor species O_3 and NO_2 measured continuously. We conclude that the low NO_3 concentrations calculated for Hyytiälä are most probably real and caused by its lower production rate as compared with that at some other sites, including Lindenberg.

Based on the comparison with the measurements during the HUMPPA-COPEC campaign in Hyytiälä, and measurements at different sites around Europe, especially the rural site in Lindenberg (Germany), we conclude that it is justified to use the calculated nitrate radical concentration.

Oxidation capacity

The oxidation capacities due to individual oxidants followed the concentration cycles of the oxidant gases (Fig. 3). There were, however, some differences in the patterns of the oxidation capacities and oxidant concentrations, as the mean reaction rate coefficients used for calculating the oxidation capacity differed between the different months due to the variable monoterpene composition. For example, the calculated NO_3 concentration was the highest in December, yet the highest oxidation capacity due to NO_3 was obtained for November when both NO_3 concentration and NO_3 reaction rate coefficient were high (Table 1).

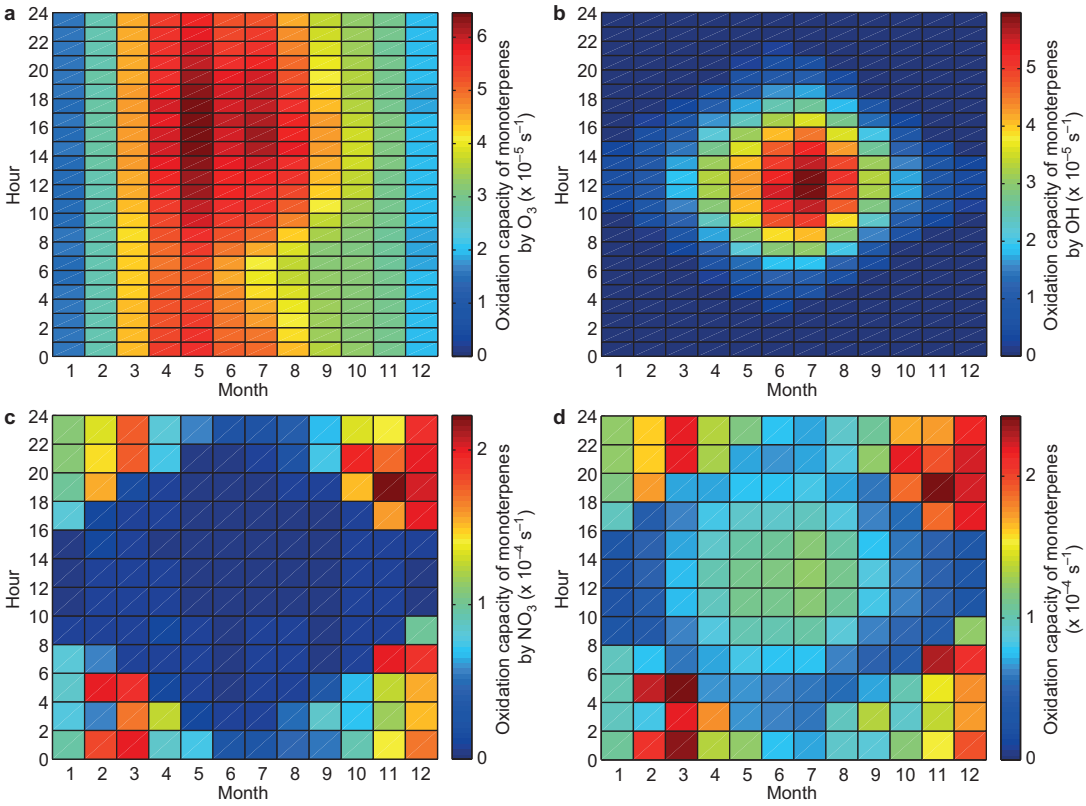

Fig. 3. Temporal variation in median oxidation capacity of monoterpenes, by (**a**) O_3, (**b**) OH, (**c**) NO_3 and (**d**) all oxidants. In figures showing the NO_3 concentration, the averaging is over two-hour interval. Note the differing colour scales.

The total oxidation capacity of monoterpenes was dominated by the nighttime peaks caused by the NO_3 in spring and autumn (Fig. 3d and c, respectively). During these times of the year, the total oxidation capacity was around 2×10^{-4} s^{-1}, of which the NO_3 accounted for around 80%. In daytime during summer, there was another peak in the oxidation capacity caused by the high oxidation capacities by OH and O_3 (Fig. 3d). This peak, however, was only half in magnitude as compared with the peaks caused by the nitrate radical during the cold season.

In addition to the absolute value of the oxidation capacity, the fraction of the oxidation capacity caused by each individual oxidant is also of interest, as it defines the fraction of monoterpenes oxidized by the individual oxidants and therefore the oxidation pathway. O_3 was the only studied oxidant present during both day and nighttime in substantial amounts, since NO_3 is mostly present during nights and OH during daylight hours. Therefore, knowing the ratio of the oxidation capacity caused by O_3 at any time is sufficient to crudely estimate the role of the other two oxidants: during night the remaining oxidation capacity is caused by NO_3 and during the day mainly by OH. From November to March, NO_3 clearly dominated the nighttime oxidation capacity, as the contribution of O_3 was mainly below 0.2 (Fig. 4). From May to September, however, the contribution of O_3 was greater, at around 0.4 or even more, and from June to August O_3 clearly dominated the nighttime oxidation capacity.

For most of the year, the daytime oxidation capacity was dominated by O_3 (Fig. 4). The highest contributions by O_3 were obtained for the morning and evening when OH and NO_3 concentration levels were low. In summer, the contributions of the OH and O_3 were almost the same during midday. It is also worth noting that

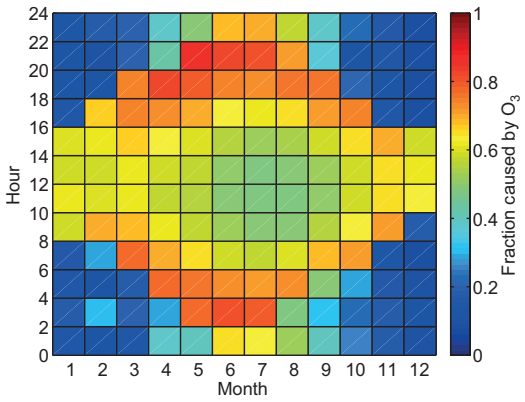

Fig. 4. Temporal variation in the median contribution of O_3 to the total oxidation capacity.

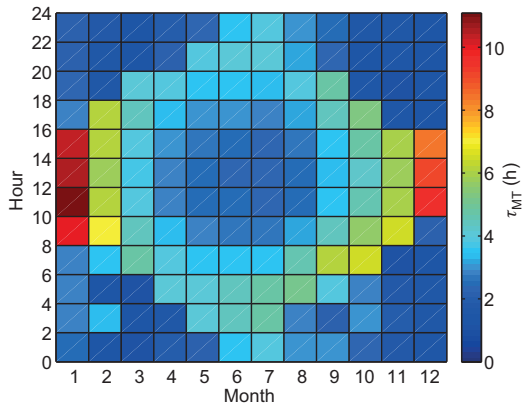

Fig. 5. Temporal variation in the median turnover time of monoterpenes.

from November to February, the contributions of OH and NO_3 to the daytime oxidation capacity were similar, as the calculated OH concentration levels were low.

Monoterpene lifetimes and concentrations

The lifetime of monoterpenes, calculated as the median of the inverse of the oxidation capacity, was a few hours and rarely exceeded five hours (Fig. 5). The longest lifetimes, around 10 hours, were obtained for daytime in December and January when the oxidation by OH and O_3 was still weak. During nights outside the summer period, the monoterpene lifetime was typically about one or two hours. The shortest lifetimes, slightly more than an hour, were obtained for the nights of March and December when the nitrate radical oxidation capacity peaked. Another minimum was obtained for daytime in summer: from June to August the shortest monoterpene lifetimes were about two hours in midday.

The median measured monoterpene concentrations were highest in summer and during nights when the planetary boundary layer was shallow and emitted compounds stayed near the ground (Fig. 6). The highest median monoterpene concentration of 1.4×10^{10} molecules cm^{-3} was observed in July between 20:00 and 22:00. In winter, monoterpene concentrations were about one order of magnitude lower than during summer nights.

Association with the particle growth rate

The calculated oxidation capacities, along with the oxidation rates and monoterpene concentrations, were compared with particle growth rates during NPF events. The medians (MD) of oxidation capacities, rates and monoterpene concentrations over three time intervals (on the night preceding the event, after the sunrise but before the particle growth, and during the particle growth of the corresponding size class) were used as the independent variables in the examination. The night was defined as the time when the UVB radiation was below 0.01 W m^{-2}. The particle growth time was assumed to start one hour before the growth was observed, and end one hour after the growth had stopped or particles had grown out of the size range. As the dependent variables, the growth rates of particles in the size ranges 1.5–3 nm, 3–7 nm and 7–20 nm during the NPF events were used. The variables were plotted against each other, both on linear and logarithmic scales, and the relations were assessed both visually from the scatter plots and using Pearson's product-moment correlation coefficients (r) calculated for the pairs (if necessary after log-transformations of the data).

When comparing any of the above quantities with the particle growth rates observed during an NPF event, it has to be kept in mind that the air mass from which these quantities were measured is not the same as the air mass where the observed particle growth took place. For example, when comparing a monoterpene concentration during

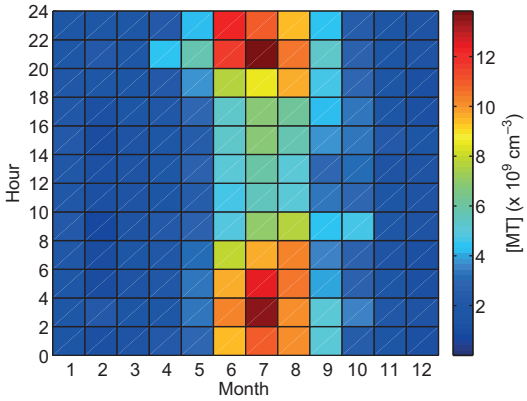

Fig. 6. Temporal variation in the median monoterpene concentration.

the preceding night with the particle growth rate during the following day, these two quantities represent measurements made from different air masses; the air mass in which the growth was measured was situated upwind of the station at the time of the monoterpene measurement. This feature limits the establishment of a cause and effect relation. However, the forest surrounding the measurement site is homogeneous for large distances (Haapanala *et al*. 2007), suggesting that the monoterpene emissions and concentrations remain relatively unchanged over large distances. This is further supported by the shape of the growing nucleation mode, which is often continuous over periods up to 12–24 hours, which can only be explained if the region around Hyytiälä is largely homogeneous. Nucleation events were proposed to take place on a regional scale already by Kulmala *et al*. (1998). We, therefore, consider Hyytiälä to be representative of the surrounding area, and assert that our approach of comparing quantities measured at different times at this single location is justified. Nevertheless, this source of uncertainty was considered throughout the analysis and interpretation of our findings.

The strongest correlation we found was that between the median oxidation rate of monoterpenes by ozone during the night preceding an NPF event and growth rate of 7–20 nm particles during the event both log-transformed (r = 0.72; Fig. 7a and Table 2). The correlation between the monoterpene concentration during the night preceding an NPF event and the growth rate of 7–20 nm particles during the event (r = 0.71) was almost as strong. None of the investigated quantities correlated strongly with the growth rates of 1.5–3 nm or 3–7 nm particles (Table 2). Therefore, hereafter the term "particle growth rate" refers to the growth rate of 7–20 nm particles, unless otherwise mentioned.

As compared with the preceding night, the median monoterpene oxidation rate by ozone both before and during growth correlated weakly with the particle growth rate (Table 2). The same was found for the monoterpene concentration. Therefore, it seems that the monoterpene concentration and oxidation rate by ozone during the nighttime were more strongly related to the particle growth rate than the same quantities during daytime.

As compared with that of the oxidation rate of monoterpenes by ozone, the correlation of the

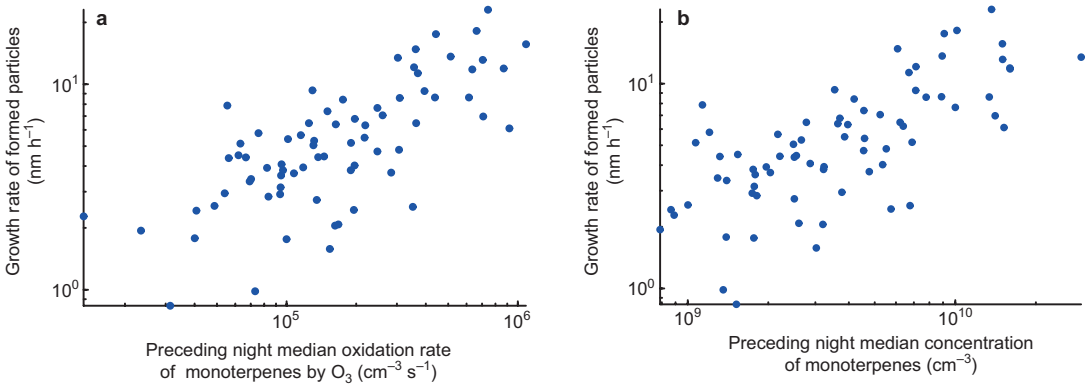

Fig. 7. Scatterplots of the growth rates of 7–20 nm particles, with (**a**) median oxidation rate of monoterpenes by O_3 during the preceding night, and (**b**) the median concentration of monoterpenes during the preceding night.

total monoterpene oxidation rate with the particle growth rate was weaker (r = 0.53–0.63; *see* Table 2). Of all the monoterpene oxidation rates, that by NO_3 during night showed the weakest correlation with the particle growth rate (r = 0.29). Out of the daytime monoterpene oxidation rates, that by OH during the growth showed the strongest correlation with the particle growth rate (r = 0.64).

As compared with the monoterpene oxidation rate or concentration, the oxidation capacity of the atmosphere showed a weaker correlation with the particle growth rate. The oxidation capacity of NO_3 generally correlated negatively with the growth particle growth rate, whereas the oxidation capacities of OH and O_3 correlated positively with it. The negative correlation between the nitrate radical oxidation capacity and particle growth rate can be due to the annual patterns of the nitrate radical and monoterpene concentrations. NO_3 concentrations are highest during the cold season when both monoterpene emissions and concentrations are small. Monoterpene concentrations correlated positively with the particle growth rate, and therefore the nitrate radical oxidation capacity correlated negatively with the particle growth rate. On the other hand, OH and O_3 concentrations showed an annual behaviour that was similar to that of monoterpenes: again, some of their correlation with the particle growth rate could be explained by this relationship.

To eliminate the effect of the oxidant concentrations correlating with monoterpene concentrations, partial correlations (i.e. the correlation of two variables, controlling for the effect of one or more other variables) were also calculated for the oxidation capacities, accounting for the correlation of the preceding night monoterpene concentration with the particle growth rate. The partial correlations of the total or individual oxidation capacities with the particle growth rate were weak to moderate. All the partial correlations of the oxidation capacities with the growth rate were positive, except for that of oxidation capacity by OH during the morning before growth, which was not statistically significant (r = –0.18, p = 0.14). The highest partial correlation was found for the oxidation capacity by OH during the particle growth (r = 0.36, $p = 3.7 \times 10^{-3}$).

The fact that the oxidation capacities themselves do not correlate strongly with the growth rate is also likely related to the fact that NPF events typically occur during clear sky conditions, when there is plenty of OH available. This supports the findings of Yli-Juuti *et al*. (2011) that the oxidant concentrations are not strongly connected to the growth rates. The differences in the correlations between oxidation rates by

Table 2. Pearson's correlation coefficient (r) between the particle growth rate during an NPF event and selected quantities, along with the number of observations (n) and the p values. The selected quantities are monoterpene concentrations ([MT]) and oxidation rates of monoterpenes (OR, both total and by different oxidants) at different times with respect to the NPF event. In the case of individual oxidants, the oxidant in question is indicated in the subscript. The particle growth rates in the diameter ranges 1.5–3 nm, 3–7 nm and 7–20 nm were considered separately. All correlations are for log-transformed data.

	1.5–3 nm			3–7 nm			7–20 nm		
	r	p	n	r	p	n	r	p	n
$[MT]_{preceding\ night}$	–0.23	0.11	47	0.27	2.4×10^{-2}	68	0.71	2.0×10^{-12}	74
$[MT]_{before\ growth}$	–0.11	0.49	42	0.24	5.6×10^{-2}	64	0.58	3.8×10^{-7}	66
$[MT]_{during\ growth}$	–0.24	0.14	41	0.08	0.54	59	0.50	1.6×10^{-5}	67
$OR_{preceding\ night}$	–0.00	0.99	45	0.40	1.0×10^{-3}	66	0.63	4.0×10^{-9}	71
$OR_{before\ growth}$	–0.05	0.77	41	0.26	4.1×10^{-2}	63	0.53	5.3×10^{-6}	64
$OR_{during\ growth}$	–0.25	0.12	38	0.11	0.41	56	0.55	2.0×10^{-6}	65
$OR_{O_3,\ preceding\ night}$	–0.19	0.21	47	0.31	9.4×10^{-3}	68	0.72	1.1×10^{-12}	73
$OR_{O_3,\ before\ growth}$	–0.06	0.72	42	0.25	4.5×10^{-2}	64	0.52	1.0×10^{-5}	65
$OR_{O_3,\ during\ growth}$	–0.19	0.23	41	0.15	0.26	59	0.56	8.6×10^{-7}	66
$OR_{OH,\ before\ growth}$	–0.03	0.84	42	0.20	0.12	64	0.54	3.6×10^{-6}	66
$OR_{OH,\ during\ growth}$	–0.27	9.4×10^{-2}	39	0.03	0.81	57	0.64	3.3×10^{-8}	60
$OR_{NO_3,\ preceding\ night}$	0.12	0.46	43	0.37	2.7×10^{-3}	64	0.29	1.6×10^{-2}	69

different oxidants suggest that the identity of the oxidant affects the growth rate. The effect of the monoterpene composition, i.e. the relative abundances of different monoterpenes, was not investigated in this study.

Discussion

Both the oxidation rate of monoterpenes by ozone and their concentration correlated strongly with the growth rate of aerosol particles. This supports the findings of Kulmala *et al*. (1998), Riipinen *et al*. (2011) and Yli-Juuti *et al*. (2011) that the oxidation of monoterpenes, i.e. the production of oxidized monoterpenes, plays an important role in the growth of atmospheric aerosol particles.

The oxidation capacity of the atmosphere in Hyytiälä is generally high enough for the turnover time of the monoterpenes to be no more than a few hours. This estimate agrees qualitatively with other studies (Kesselmeier and Staudt 1999, Atkinson and Arey 2003, Laothawornkitkul *et al*. 2009). This also means that over a relatively short time scale, on the order of hours, the production and removal of monoterpenes are expected to become roughly equal. Hence, an increase in the oxidation capacity increases the oxidation rate of the monoterpenes only temporarily, as monoterpenes will be depleted from the atmosphere and this in turn will lower the oxidation rate. Similarly, if the oxidation capacity is lowered, the monoterpene oxidation rate will slow down only until enough monoterpenes have been accumulated to increase the oxidation rate again. There was only a weak to moderate correlation between the oxidation capacity and particle growth rate, even though monoterpene oxidation seems to have a significant effect on the particle growth rate. Taken together, the above findings suggest that the oxidation of monoterpenes over Hyytiälä is not limited by the availability of oxidants in the atmosphere, but rather by monoterpene emissions, which supports the findings of Yli-Juuti *et al*. (2011).

The particle growth rate seemed to be tied more closely to the monoterpene oxidation rate by ozone and monoterpene concentration during the preceding night than to the same quantities during daytime, judged both from the correlation coefficients and visual inspection of the scatter plots. The planetary boundary layer grows between the preceding night and an NPF event, causing dilution of the boundary-layer air that varies from day to day. The variability of such dilution, and possibly some other factors, are expected to weaken the correlation between the monoterpene concentration during the previous night and particle growth rate during an NPF event. The fact that these two quantities correlated strongly with each other despite the dilution effect suggests that some process during the preceding night plays a very important role in the particle growth during an NPF event.

One explanation of how the processes occurring during the preceding night might be related to the particle growth during an NPF event relates to the potential build-up of the concentrations of monoterpenes which have been primarily (i.e. once) oxidized. These first-generation oxidation products are expected to be less volatile than monoterpenes, yet mainly too volatile to condense efficiently onto particles. Any first-generation oxidation product resulting from nighttime oxidation that condenses already during night cannot contribute to the particle growth during an NPF event. The further the oxidation proceeds, the higher the total yield of condensable products (for example ELVOCs, extremely low volatility organic compounds, Donahue *et al*. 2012) is. Many of the first-generation monoterpene oxidation products of ozone cannot be oxidized further by ozone because the double bond between carbon atoms has been lost and this double bond is the only place where ozone can react (Vereecken and Francisco 2012). Nitrate radical can react both by attacking the double bond and by H-abstraction (Sadanaga *et al*. 2003, Vereecken and Francisco 2012). However, the reaction by H-abstraction is negligible as compared with the addition to the double bond (Atkinson 1997), and therefore the nitrate radical does not react efficiently with these first-generation oxidation products from the ozone oxidation. Therefore, there may be a nighttime build-up in the atmosphere of the primarily-oxidized monoterpenes which cannot, or can only very slowly, be oxidized further by ozone or the nitrate radical. Then, when the sun

rises and the boundary layer expands, the OH radical concentration rises. The oxidation by OH does not rely only on the double bond as it takes place also through H-abstraction. Therefore, the primarily-oxidized compounds which have been accumulating during night can now be oxidized by OH. Since these compounds are already primarily oxidized, the resulting oxidation products have a lower volatility than the first-generation oxidation products resulting from oxidation of monoterpenes by OH. These, or compounds oxidized even further by OH, may then condense onto newly-formed particles and enhance their growth. If these primarily-oxidized species accumulate sufficiently during night, they might have a larger role in the particle growth than the monoterpenes oxidized during an NPF event. The strong correlations of both monoterpene concentration and monoterpene oxidation rate by ozone during the preceding night with the particle growth rate supports the above scenario. The monoterpene oxidation rate by OH during the particle growth correlated more strongly with the particle growth rate than did any other daytime quantity. This also supports the idea that it is the OH radical that is oxidizing the primarily-oxidised compounds further.

One product of the monoterpene oxidation by ozone is the stabilized Criegee intermediate (sCI, Mauldin *et al*. 2012). The sCI has two free radical sites and can possibly act as an oxidant for monoterpenes. Therefore, the sCI could also be involved in the reactions following monoterpene oxidation by ozone. The reaction rate of the sCI with monoterpenes and its atmospheric lifetime are still poorly known.

Summary and conclusions

The temporal variation in the oxidant gases O_3, OH and NO_3, as well as the oxidation capacity caused by these oxidants, were investigated at the SMEAR II station in a boreal coniferous forest ecosystem. We found that for most of the year, the nighttime and daytime oxidation capacities are dominated by NO_3 and O_3, respectively. The oxidation capacity was found to be higher during night than day for most of the year as well. However, from June to August, O_3 dominated the nighttime oxidation capacity and the highest oxidation capacity was observed in midday when the contributions of OH and O_3 to this oxidation capacity were almost equal.

The atmospheric lifetime of monoterpenes in the pine forest was found to be relatively short, in the order of hours. For most of the year, the shortest monoterpene lifetimes were observed during night with values typically between about one and two hours. In summer, the monoterpene lifetime was shortest at around midday.

A strong correlation was found between the median oxidation rate of monoterpenes by ozone during the night preceding an NPF event, and the growth rate of 7–20 nm particles during the event. For the growth rates of particles smaller than 7 nm in diameter, the correlations were moderate or weak. The median concentration of monoterpenes during the night preceding the event was also strongly correlated with the growth rate of 7–20 nm particles. The oxidant concentrations themselves, or the oxidation capacity, did not show any notable correlations with the particle growth rate. Of the daytime quantities investigated, the monoterpene oxidation rate by OH showed the strongest correlation with the growth rate of 7–20 nm particles. Since the particle growth rate correlated more strongly with the monoterpene oxidation rate by ozone and monoterpene concentration during the previous night than with the same quantities during daytime, it seems that the particle growth rate is affected by what happens during the previous night. A possible explanation for this might be the build-up of relatively high-volatility first-generation oxidation products during night, which are oxidized further by OH during daytime, after which they can then contribute to the particle growth.

Our results support the earlier findings that at this site, and possibly in the boreal forest in general, monoterpene oxidation products play a significant role in the atmospheric nanoparticle growth. Furthermore, it seems that the formation of condensable oxidation products is mainly limited by the emissions of monoterpenes, and not by the availability of oxidants.

Acknowledgements: We would like to thank Michael Boy for constructive discussions related to the calculation of the nitrate radical concentration. This research was supported by the Academy of Finland (Centre of Excellence program, pro-

ject number 127534), and by the Nordic Top-level Research Initiative (TRI) Cryosphere-Atmosphere Interactions in a Changing Arctic Climate (CRAICC).

References

Aalto P., Hämeri K., Becker E., Weber R., Salm J., Mäkelä J., Hoell C., O'Dowd C., Karlsson H., Hansson H., Väkevä M., Koponen I., Buzorius G. & Kulmala M. 2001. Physical characterization of aerosol particles during nucleation events. *Tellus* 53B: 344–358.

Allan B., McFiggans G., Plane J., Coe H. & McFadyen G. 2000. The nitrate radical in the remote marine boundary layer. *J. Geophys. Res.* 105: 24191–24204.

Atkinson R. 1997. Gas-phase tropospheric chemistry of volatile organic compounds: 1. Alkanes and alkenes. *J. Phys. Chem. Ref. Data* 26: 215–290.

Atkinson R. & Arey J. 2003. Gas-phase tropospheric chemistry of biogenic volatile organic compounds: a review. *Atmos. Environ.* 37: S197–S219.

Bäck J., Aalto J., Henriksson M., Hakola H., He Q. & Boy M. 2012. Chemodiversity of a Scots pine stand and implications for terpene air concentrations. *Biogeosciences* 9: 689–702.

de Gouw J. & Warneke C. 2007. Measurements of volatile organic compounds in the Earth's atmosphere using proton-transfer-reaction mass spectrometry. *Mass Spectrom. Rev.* 26: 223–257.

de Gouw J., Goldan P., Warneke C., Kuster W., Roberts J., Marchewka M., Bertman S., Pszenny A. & Keene W. 2003. Validation of proton transfer reaction-mass spectrometry (PTR-MS) measurements of gas-phase organic compounds in the atmosphere during the New England Air Quality Study (NEAQS) in 2002. *J. Geophys. Res.* 108, D21, doi:10.1029/2003JD003863.

Dlugokencky E. & Howard C. 1989. Studies of NO_3 radical reactions with some atmospheric organic-compounds at low-pressures. *J. Phys. Chem.* 93: 1091–1096.

Donahue N.M., Kroll J.H., Pandis S.N. & Robinson A.L. 2012. A two-dimensional volatility basis set — Part 2: Diagnostics of organic-aerosol evolution. *Atmos. Chem. Phys.* 12: 615–634.

Geyer A., Ackermann R., Dubois R., Lohrmann B., Müller T. & Platt U. 2001a. Long-term observation of nitrate radicals in the continental boundary layer near Berlin. *Atmos. Environ.* 35: 3619–3631.

Geyer A., Alicke B., Konrad S., Schmitz T., Stutz J. & Platt U. 2001b. Chemistry and oxidation capacity of the nitrate radical in the continental boundary layer near Berlin. *J. Geophys. Res.* 106: 8013–8025.

Ghirardo A., Koch K., Taipale R., Zimmer I., Schnitzler J.-P. & Rinne J. 2010. Determination of de novo and pool emissions of terpenes from four common boreal/alpine trees by $^{13}CO_2$ labelling and PTR-MS analysis. *Plant Cell Environ.* 33: 781–792.

Guenther A.B., Jiang X., Heald C.L., Sakulyanontvittaya T., Duhl T., Emmons L.K. & Wang X. 2012. The model of emissions of gases and aerosols from nature version 2.1 (MEGAN2.1): an extended and updated framework for modeling biogenic emissions. *Geosci. Model Dev.* 5: 1471–1492.

Haapanala S., Rinne J., Hakola H., Hellén H., Laakso L., Lihavainen H., Janson R., O'Dowd C. & Kulmala M. 2007. Boundary layer concentrations and landscape scale emissions of volatile organic compounds in early spring. *Atmos. Chem. Phys.* 7: 1869–1878.

Hakola H., Hellén H., Hemmilä M., Rinne J. & Kulmala M. 2012. In situ measurements of volatile organic compounds in a boreal forest. *Atmos. Chem. Phys.* 12: 11665–11678.

Hari P. & Kulmala M. 2005. Station for Measuring Ecosystem–Atmosphere Relations (SMEAR II). *Boreal Env. Res.* 10: 315–322.

Hirsikko A., Laakso L., Hõrrak U., Aalto P., Kerminen V.-M. & Kulmala M. 2005. Annual and size dependent variation of growth rates and ion concentrations in boreal forest. *Boreal Env. Res.* 10: 357–369.

Ilvesniemi H., Pumpanen J., Duursma R., Hari P., Keronen P., Kolari P., Kulmala M., Mammarella I., Nikinmaa E., Rannik Ü., Pohja T., Siivola E. & Vesala T. 2010. Water balance of a boreal Scots pine forest. *Boreal Env. Res.* 15: 375–396.

Isidorov V., Zenkevich I. & Ioffe B. 1985. Volatile organic compounds in the atmosphere of forests. *Atmos. Environ.* 19: 1–8.

Jenkin M., Saunders S., Wagner V. & Pilling M. 2003. Protocol for the development of the Master Chemical Mechanism, MCM v3 (Part B): tropospheric degradation of aromatic volatile organic compounds. *Atmos. Chem. Phys.* 3: 181–193.

Kerminen V.-M., Paramonov M., Anttila T., Riipinen I., Fountoukis C., Korhonen H., Asmi E., Laakso L., Lihavainen H., Swietlicki E., Svenningsson B., Asmi A., Pandis S.N., Kulmala M. & Petäjä T. 2012. Cloud condensation nuclei production associated with atmospheric nucleation: a synthesis based on existing literature and new results. *Atmos. Chem. Phys.* 12: 12037–12059.

Kesselmeier J. & Staudt M. 1999. Biogenic volatile organic compounds (VOC): an overview on emission, physiology and ecology. *J. Atmos. Chem.* 33: 23–88.

Kolari P., Bäck J., Taipale R., Ruuskanen T.M., Kajos M.K., Rinne J., Kulmala M. & Hari P. 2012. Evaluation of accuracy in measurements of VOC emissions with dynamic chamber system. *Atmos. Environ.* 62: 344–351.

Kulmala M., Riipinen I., Sipilä M., Manninen H.E., Petäjä T., Junninen H., Dal Maso M.D., Mordas G., Mirme A., Vana M., Hirsikko A., Laakso L., Harrison R.M., Hanson I., Leung C., Lehtinen K.E.J. & Kerminen V.-M. 2007. Toward direct measurement of atmospheric nucleation. *Science* 318: 89–92.

Kulmala M., Toivonen A., Mäkelä J. & Laaksonen A. 1998. Analysis of the growth of nucleation mode particles observed in boreal forest. *Tellus* 50B: 449–462.

Kulmala M., Vehkamäki H., Petäjä T., Dal Maso M., Lauri A., Kerminen V., Birmili W. & McMurry P. 2004. Formation and growth rates of ultrafine atmospheric particles: a review of observations. *J. Aerosol Sci.* 35: 143–176.

Laothawornkitkul J., Taylor J.E., Paul N.D. & Hewitt C.N. 2009. Biogenic volatile organic compounds in the Earth system. *New Phytologist* 183: 27–51.

Leppä J., Anttila T., Kerminen V.M., Kulmala M. & Lehtinen K.E.J. 2011. Atmospheric new particle formation: real and apparent growth of neutral and charged particles. *Atmos. Chem. Phys.* 11: 4939–4955.

Leppä J., Gagné S., Laakso L., Manninen H.E., Lehtinen K.E.J., Kulmala M. & Kerminen V.-M. 2013. Using measurements of the aerosol charging state in determination of the particle growth rate and the proportion of ion-induced nucleation. *Atmos. Chem. Phys.* 13: 463–486.

Lindinger W., Hansel A. & Jordan A. 1998. Proton-transfer-reaction mass spectrometry (PTR-MS): on-line monitoring of volatile organic compounds at pptv levels. *Chem. Soc. Rev.* 27: 347–354.

Litvak M., Madronich S. & Monson R. 1999. Herbivore-induced monoterpene emissions from coniferous forests: Potential impact on local tropospheric chemistry. *Ecol. Appl.* 9: 1147–1159.

Mauldin R.L.III, Berndt T., Sipilä M., Paasonen P., Petäjä T., Kim S., Kurten T., Stratmann F., Kerminen V.-M. & Kulmala M. 2012. A new atmospherically relevant oxidant of sulphur dioxide. *Nature* 488: 193–196.

Mirme A., Tamm E., Mordas G., Vana M., Uin J., Mirme S., Bernotas T., Laakso L., Hirsikko A. & Kulmala M. 2007. A wide-range multi-channel air ion spectrometer. *Boreal Env. Res.* 12: 247–264.

Orlando J., Tyndall G., Moortgat G. & Calvert J. 1993. Quantum yields for NO_3 photolysis between 570 and 635 nm. *J. Phys. Chem.* 97: 10996–11000.

Osthoff H.D., Pilling M.J., Ravishankara A.R. & Brown S.S. 2007. Temperature dependence of the NO_3 absorption cross-section above 298 K and determination of the equilibrium constant for $NO_3 + NO_2 \leftrightarrow N_2O_5$ at atmospherically relevant conditions. *Phys. Chem. Chem. Phys.* 9: 5785–5793.

Paasonen P., Asmi A., Petäjä T., Kajos M.K., Äijälä M., Junninen H., Holst T., Abbatt J.P.D., Arneth A., Birmili W., van der Gon H.D., Hamed A., Hoffer A., Laakso L., Laaksonen A., Leaitch W.R., Plass-Dülmer C., Pryor S.C., Räisänen P., Swietlicki E., Wiedensohler A., Worsnop D.R., Kerminen V.-M. & Kulmala M. 2013. Warming induced increase in aerosol number concentration likely to moderate climate change. *Nature Geosci.* 6: 438–442.

Petäjä T., Mauldin R.L.III, Kosciuch E., McGrath J., Nieminen T., Paasonen P., Boy M., Adamov A., Kotiaho T. & Kulmala M. 2009. Sulfuric acid and OH concentrations in a boreal forest site. *Atmos. Chem. Phys.* 9: 7435–7448.

Riipinen I., Pierce J.R., Yli-Juuti T., Nieminen T., Häkkinen S., Ehn M., Junninen H., Lehtipalo K., Petäjä T., Slowik J., Chang R., Shantz N.C., Abbatt J., Leaitch W.R., Kerminen V. M., Worsnop D.R., Pandis S.N., Donahue N.M. & Kulmala M. 2011. Organic condensation: a vital link connecting aerosol formation to cloud condensation nuclei (CCN) concentrations. *Atmos. Chem. Phys.* 11: 3865–3878.

Riipinen I., Yli-Juuti T., Pierce J.R., Petäjä T., Worsnop D.R., Kulmala M. & Donahue N.M. 2012. The contribution of organics to atmospheric nanoparticle growth. *Nature Geosci.* 5: 453–458.

Rinne J., Bäck J. & Hakola H. 2009. Biogenic volatile organic compound emissions from the Eurasian taiga: current knowledge and future directions. *Boreal Env. Res.* 14: 807–826.

Rinne J., Markkanen T., Ruuskanen T.M., Petäjä T., Keronen P., Tang M.J., Crowley J.N., Rannik Ü. & Vesala T. 2012. Effect of chemical degradation on fluxes of reactive compounds — a study with a stochastic Lagrangian transport model. *Atmos. Chem. Phys.* 12: 4843–4854.

Rinne J., Taipale R., Markkanen T., Ruuskanen T.M., Hellén H., Kajos M.K., Vesala T. & Kulmala M. 2007. Hydrocarbon fluxes above a Scots pine forest canopy: measurements and modeling. *Atmos. Chem. Phys.* 7: 3361–3372.

Röhrer F. & Berresheim H. 2006. Strong correlation between levels of tropospheric hydroxyl radicals and solar ultraviolet radiation. *Nature* 442: 184–187.

Sadanaga Y., Matsumoto J. & Kajii Y. 2003. Photochemical reactions in the urban air: Recent understandings of radical chemistry. *J. Photochem. Photobiol. C* 4: 85–104.

Saunders S., Jenkin M., Derwent R. & Pilling M. 2003. Protocol for the development of the Master Chemical Mechanism, MCM v3 (Part A): tropospheric degradation of non-aromatic volatile organic compounds. *Atmos. Chem. Phys.* 3: 161–180.

Sipilä M., Berndt T., Petäjä T., Brus D., Vanhanen J., Stratmann F., Patokoski J., Mauldin R.L.III, Hyvärinen A.-P., Lihavainen H. & Kulmala M. 2010. The role of sulfuric acid in atmospheric nucleation. *Science* 327: 1243–1246.

Taipale R., Kajos M.K., Patokoski J., Rantala P., Ruuskanen T.M. & Rinne J. 2011. Role of de novo biosynthesis in ecosystem scale monoterpene emissions from a boreal Scots pine forest. *Biogeosciences* 8: 2247–2255.

Taipale R., Ruuskanen T.M., Rinne J., Kajos M.K., Hakola H., Pohja T. & Kulmala M. 2008. Technical Note: Quantitative long-term measurements of VOC concentrations by PTR-MS — measurement, calibration, and volume mixing ratio calculation methods. *Atmos. Chem. Phys.* 8: 6681–6698.

Tammet H. 2006. Continuous scanning of the mobility and size distribution of charged clusters and nanometer particles in atmospheric air and the Balanced Scanning Mobility Analyzer BSMA. *Atmos. Res.* 30: 523–535.

Tunved P., Hansson H., Kerminen V., Ström J., Dal Maso M., Lihavainen H., Viisanen Y., Aalto P., Komppula M. & Kulmala M. 2006. High natural aerosol loading over boreal forests. *Science* 312: 261–263.

Vereecken L. & Francisco J.S. 2012. Theoretical studies of atmospheric reaction mechanisms in the troposphere. *Chem. Soc. Rev.* 41: 6259–6293.

Vrekoussis M., Kanakidou M., Mihalopoulos N., Crutzen P., Lelieveld J., Perner D., Berresheim H. & Baboukas E. 2004. Role of the NO_3 radicals in oxidation processes in the eastern Mediterranean troposphere during the MINOS campaign. *Atmos. Chem. Phys.* 4: 169–182.

Warneke C., De Gouw J., Kuster W., Goldan P. & Fall R. 2003. Validation of atmospheric VOC measurements by proton-transfer-reaction mass spectrometry using a gas-chromatographic preseparation method. *Environ. Sci. Technol.* 37: 2494–2501.

Williams J., Crowley J., Fischer H., Harder H., Martinez M., Petäjä T., Rinne J., Bäck J., Boy M., Dal Maso M., Hakala J., Kajos M., Keronen P., Rantala P., Aalto J., Aaltonen H., Paatero J., Vesala T., Hakola H., Levula J., Pohja T., Herrmann F., Auld J., Mesarchaki E., Song W., Yassaa N., Nölscher A., Johnson A.M., Custer T., Sinha V., Thieser J., Pouvesle N., Taraborrelli D., Tang M.J., Bozem H., Hosaynali-Beygi Z., Axinte R., Oswald R., Novelli A., Kubistin D., Hens K., Javed U., Trawny K., Breitenberger C., Hidalgo P.J., Ebben C.J., Geiger F.M., Corrigan A.L., Russell L.M., Ouwersloot H.G., Vilà-Guerau de Arellano J., Ganzeveld L., Vogel A., Beck M., Bayerle A., Kampf C.J., Bertelmann M., Köllner F., Hoffmann T., Valverde J., González D., Riekkola M.L., Kulmala M. & Lelieveld J. 2011. The summertime boreal forest field measurement intensive (HUMPPA-COPEC-2010): an overview of meteorological and chemical influences. *Atmos. Chem. Phys.* 11: 10599–10618.

Yli-Juuti T., Nieminen T., Hirsikko A., Aalto P.P., Asmi E., Hõrrak U., Manninen H.E., Patokoski J., Dal Maso M., Petäjä T., Rinne J., Kulmala M. & Riipinen I. 2011. Growth rates of nucleation mode particles in Hyytiälä during 2003–2009: variation with particle size, season, data analysis method and ambient conditions. *Atmos. Chem. Phys.* 11: 12865–12886.